Melting of *Saccharomyces cerevisiae* 5S Ribonucleic Acid: Ultraviolet Absorption, Circular Dichroism, and 360-MHz Proton Nuclear Magnetic Resonance Spectroscopy†

Greg A. Luoma,‡ Phillip D. Burns, Robert E. Bruce,§ and Alan G. Marshall*

ABSTRACT: The heat-induced melting of yeast 5S RNA and $tRNA^{Phe}$ has been monitored by UV, CD, and 360-MHz ^1H NMR spectroscopy in order to determine the extent of base stacking and base pairing in the native and denatured structures. In the presence of Mg^{2+}, the optical data indicate ≤40 base pairs in native yeast 5S RNA, a 60:40 ratio of GC to AU base pairs, with more single-stranded stacking and a slightly less stable structure (half-melted at 67 °C) than for $tRNA^{Phe}$ (half-melted at 71 °C). In the absence of Mg^{2+}, the NMR results identify a minimum of ~32 base pairs at 25 °C (increasing to a minimum of ~35 base pairs in the presence of Mg^{2+}), of which more than half are still intact at 48 °C. The native structure (25 °C) shows only minor dependence upon Mg^{2+} concentration, and no denatured forms could be detected. Finally, the present results support a previously proposed cloverleaf secondary structure for eukaryotic 5S RNA.

One 5S RNA molecule is a structural constituent of every studied prokaryotic and eukaryotic ribosome (Erdmann, 1976; Monier, 1974; Wool, 1979; Wittman, 1979). Prokaryotic 5S RNA is implicated in binding of all tRNAs to the ribosome (Erdmann, 1976; Sprinzl et al., 1976; Swarz et al., 1976), while eukaryotic 5S RNA is thought to participate in the ribosomal binding of initiator tRNA only (Erdmann, 1976).

Many previous studies have characterized the optical properties of various tRNAs and of *pro*karyotic 5S RNA (Romer et al., 1970; Fresco et al., 1963; Riesner et al., 1973; Levy et al., 1972; Levy & Rialdi, 1972; Chen et al., 1978; Cantor, 1968; Boedtker & Kelling, 1967; Scott et al., 1968; Cramer & Erdmann, 1968; Aubert et al., 1968; Richards et al., 1972, 1973; Gray & Saunders, 1973; Bear et al., 1977; Fox & Wong, 1978; Nazar et al., 1978; Appel et al., 1979). Moreover, since the X-ray crystal structure is refined to 2.8 Å (Sussman et al., 1978), the effects of base stacking upon the *optical* properties of $tRNA^{Phe}$ (and other tRNAs) *in solution* may be calibrated against the known stacking in the crystal structure (see below). Such comparisons give highly consistent results for tRNAs in solution and are expected to provide reliable estimates for base stacking in other RNAs (as in this work).

For prokaryotic 5S RNA, optical studies have suggested a high degree of base pairing and a largely double helical configuration; these facts are incompatible with most previously proposed secondary structural models for prokaryotic 5S RNA (Erdmann, 1976). Such studies also indicate the presence of two distinguishable conformers of *Escherichia coli* 5S RNA, whose relative proportions depend on the presence or absence of Mg^{2+} (Aubert et al., 1968; Richards et al., 1973; Weidner et al., 1977). Only the native (or "A" form) of *E. coli* 5S RNA can be reconstituted back in the ribosome (Erdmann, 1976). Interpretation of preliminary 300-MHz ^1H NMR spectra of *E. coli* 5S RNA (Kearns & Wong, 1974) is complicated by multiple conformers, poor spectral resolution, and possible aggregation at the high concentrations that were then necessary to obtain useful signal-to-noise ratios. Recent 400-MHz ^1H NMR studies of *E. coli* 5S RNA now give a consistent structural picture (Burns et al., 1980).

On the basis primarily of Raman results, we recently proposed new cloverleaf models for the secondary structures of both prokaryotic (Luoma & Marshall, 1978a) and eukaryotic (Luoma & Marshall, 1978b) 5S RNA. These structures can be made homologous for all published primary sequences of prokaryotic 5S RNA and eukaryotic 5S RNA and 5.8S RNA (Marshall et al., unpublished results) and are consistent with all previously reported physical properties as well as subsequently published chemical modification (Noller & Garrett, 1979; Nishikawa & Takemura, 1978), nuclease digestion (Nichols & Welder, 1979), infrared spectroscopy (Appel et al., 1979), optical (Maruyama et al., 1979), Raman (Chen et al., 1978), and ^{19}F NMR (Marshall & Smith, 1980) results.

For eukaryotic 5S RNA, few optical studies have been attempted and no attempts to identify multiple conformational forms have been made (Maruyama, 1979). The only reported ^1H NMR investigation (of yeast 5S RNA) was at a relatively low applied magnetic field (220 MHz) and provided resolution too poor to permit meaningful analysis of the spectrum (Wong et al., 1972). In the present study, we therefore report UV, CD, and 360-MHz ^1H NMR results for yeast 5S RNA in the presence and absence of Mg^{2+}. The optical spectra are compared to those for $tRNA^{Phe}$ (isolated from the same cells) under identical conditions in order to provide for direct calibration of the 5S RNA optical results.

Experimental Section

Isolation of 5S RNA and $tRNA^{Phe}$. 5S RNA was isolated as previously described (Luoma & Marshall, 1978b). In brief, yeast cells were first extracted with phenol and the mixed RNAs then precipitated from the aqueous layer with ethanol. The RNA was then chromatographed on DEAE-cellulose, and the 5S RNA and tRNA components were separated by using Sephadex G-100 column chromatography, then pooled, desalted, and lyophilized. Purified RNA was stored at −20 °C and tested for homogeneity by using 10% gel slab electrophoresis [method of Rubin (1973)]; under those conditions, purified yeast 5S RNA migrated as a single band.

† From the Departments of Chemistry and Biochemistry, The Ohio State University, Columbus, Ohio 43210. *Received March 25, 1980.* This work was supported by grants (to A.G.M.) from the Natural Sciences and Engineering Research Council of Canada (A-6178), the Alfred P. Sloan Foundation, and The Ohio State University.

* Alfred P. Sloan Research Fellow, 1976–1980.

‡ Present address: Defence Research Establishment Pacific, Esquimalt, B.C., Canada.

§ Present address: Open Learning Institute of B.C., Richmond, B.C., Canada.

0006-2960/80/0419-5456$01.00/0

tRNA^{Phe} was separated from the remaining mixed tRNAs by combining the procedures of Gillam et al. (1967) and Holmes et al. (1975). Purified mixed tRNA from the Sephadex G-100 fractionation was applied to a BD-cellulose (Whatman) column, and the fractions eluted using 1.0 M NaCl and 10 mM $MgCl_2$ in 10% ethanol were combined and precipitated with ethanol. This crude tRNA^{Phe} was then purified further by using a reverse salt gradient on Sepharose 4B (Holmes et al., 1975). Both the A_{260} and the fluorescence of the eluting fractions were monitored, and the peak containing the fluorescent material was isolated, desalted, and lyophilized. This fraction gave a single, sharp band on electrophoresis (10% gel slab as described above) and exhibited a [^{14}C]phenylalanine acceptance of >1600 pmol/A_{260} unit.

Preparation of Mg^{2+}-Containing and Mg^{2+}-Deficient 5S RNA and tRNA^{Phe}. For Mg^{2+}-containing samples, 5S RNA or tRNA^{Phe} was dissolved in 10 mM phosphate, pH 7, containing 100 mM NaCl and 10 mM $MgCl_2$. For Mg^{2+}-deficient samples, 5S RNA or tRNA^{Phe} was dissolved in 10 mM phosphate, pH 7, containing 100 mM NaCl and 15 mM Na_2EDTA. The solution was then heated to 65 °C for 5 min, cooled to room temperature, and dialyzed twice at 4 °C against 100 volumes of 10 mM phosphate, pH 7, containing 100 mM NaCl and 1 mM Na_2EDTA.

Renatured 5S RNA was prepared from a Mg^{2+}-deficient sample by adding solid $MgCl_2$ to a concentration of 10 mM. The RNA was then heated to 65 °C for 5 min and allowed to cool slowly to room temperature. In all the above procedures, the buffer was degassed by boiling immediately before use to prevent bubble formation during sample heating.

Ultraviolet Absorption and Circular Dichroism Measurements. All UV–melting experiments were performed by using a Cary 15 spectrophotometer equipped with a hollow cell holder. The temperature was controlled with a Haacke temperature bath and the sample temperature monitored with a YSI telethermometer with a thermistor probe inserted directly into the sample cuvette through a hole in the cap. A_{260} or A_{280} measurements were recorded at 2 °C increments, and the rate of heating was maintained at 1 °C/min.

All CD experiments were performed on a JASCO J-20 spectrometer equipped with a temperature-regulated cell block. Samples were heated at a rate of 10 °C/h, and spectra were recorded every 5 °C. The $A_{260}^{20°C}$ values for both the CD and UV experiments were adjusted to 0.7–0.8.

360-MHz ^{1}H NMR Spectra. ^{1}H NMR spectra were obtained from a Nicolet 360-MHz FT-NMR spectrometer with the kind cooperation of Professor G. N. La Mar and Dr. G. Matson at the University of California, Davis. Suppression of the strong H_2O solvent peak was achieved by using a "Redfield 21412" excitation pulse sequence (Redfield et al., 1975) whose total duration was 352.5 μs, with the excitation frequency centered 2840 Hz from the H_2O peak (i.e., centered at 12.6 ppm from DSS at 25 °C). Detection parameters were 8K FID data size, 340-ms acquisition time, spectral width ±6024 Hz, quadrature detection with phase alternation sequence, 0.75-s delay between successive acquisitions, and exponential apodization of FID equivalent to 6.00-Hz line broadening. Simulations were produced by using a Bruker Aspect 2000 computer. No base line flattening or smoothing of experimental spectra was used.

Results

UV Absorption Spectra of Yeast 5S RNA and tRNA^{Phe}. (1) 10 mM Mg^{2+} Present. Figure 1 shows the UV–melting profiles (A_{260} vs. temperature) for both yeast 5S RNA and tRNA^{Phe}. Table I lists the hypochromism (H), half-melted

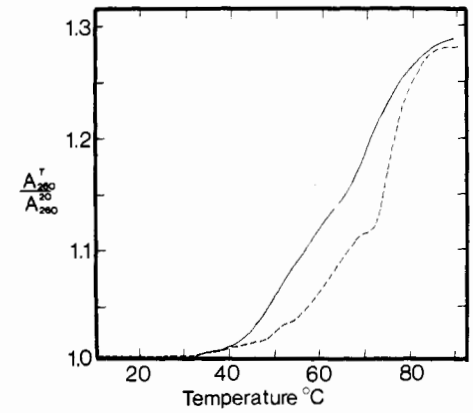

FIGURE 1: Ultraviolet absorption–melting profiles (normalized to unit absorbance at 260 nm at 20 °C) for *S. cerevisiae* 5S RNA (—) and tRNA^{Phe} (- - -) in 10 mM phosphate buffer (pH 7.0) containing 100 mM NaCl and 10 mM $MgCl_2$.

Table I: Parameters from UV Absorption–Melting Profiles for Yeast RNA

RNA type	Mg^{2+}	H^a	$T_m{}^b$ (°C)	δ^c (°C)
5S RNA	present	0.22	66	21
	removed	0.20	48	18.5
	readded	0.21	65	20
tRNA^{Phe}	present	0.22	73.5	16
	removed	0.17	44.5	18

[a] H is the total hypochromism [i.e., change in A_{260} between 25 °C (folded RNA conformation) and 86 °C (unfolded)], from Figures 1 and 4 and additional data. [b] T_m is the temperature at which the hypochromism has reached half of the total hypochromism. [c] δ is the temperature range over which the hypochromism changes from 25 to 75% of its total value.

temperature (T_m), and melting range (δ), determined from the curves of Figure 1. Because the solution conformation of yeast tRNA^{Phe} is known (Reid & Robillard, 1975), we can form definite structural conclusions about yeast 5S RNA by comparison of the optical results for 5S RNA and tRNA^{Phe}.

First, the total hypochromism (i.e., change in A_{260} on unfolding of the secondary and tertiary RNA structure) for 5S RNA is identical with that for tRNA^{Phe}. Since total hypochromism has previously been shown to give a direct and accurate measure of total base stacking and base pairing in tRNAs (Fresco et al., 1963; Boedtker & Kelling, 1967; Van et al., 1977), the yeast 5S RNA structure must therefore be as extensively base stacked and base paired as is tRNA^{Phe} (Sussman et al., 1978).

Second, T_m is 7.5 °C lower for 5S RNA than for tRNA^{Phe}. Thus, even though the two molecules exhibit similar overall degrees of base stacking and base pairing, the tRNA^{Phe} higher order structure is evidently significantly more thermodynamically stable.

The above two results can be understood from the third parameter from Figure 1, the melting range (δ), which is the temperature range over which the hypochromism increases from 25 to 75% of its total value. δ has been shown to reflect the amount of *single-stranded stacking* that contributes to the total hypochromism (Boedtker & Kelling, 1967). Therefore, 5S RNA (larger δ) probably contains more single-stranded stacking than tRNA^{Phe} does (smaller δ), giving rise to a less stable structure with the same total hypochromism.

Finally, the UV–melting profile (Figure 1) for yeast 5S RNA is biphasic, while that for tRNA^{Phe} appears multiphasic. The biphasic 5S RNA profile observed here differs from previous reports (Maruyama et al., 1979; Wong et al., 1972). However, one of these studies (Wong et al., 1972) employed

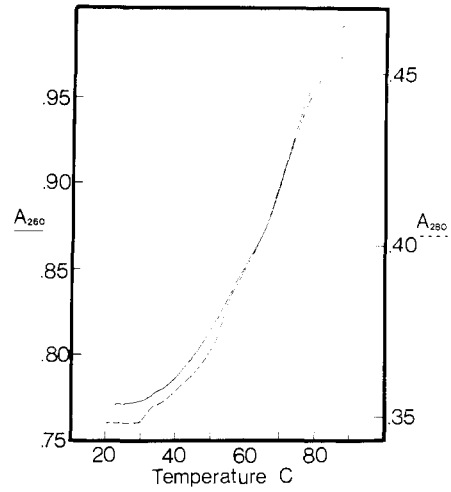

FIGURE 2: Experimental ultraviolet absorption–melting profiles for *S. cerevisiae* 5S RNA at 260 nm (—) and at 280 nm (---). Buffer was as for Figure 1.

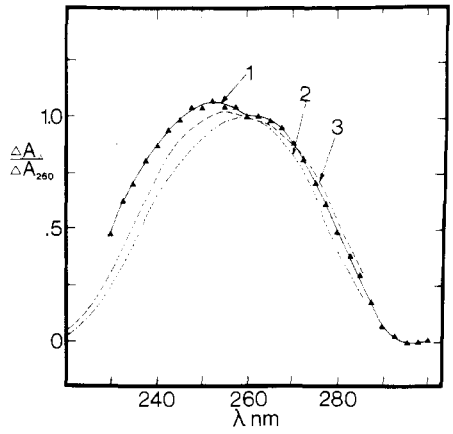

FIGURE 3: Normalized hypochromism spectra. (1) Experimental *S. cerevisiae* 5S RNA; (2) theoretical spectrum for 50:50 ratio of AU to GC pairs; (3) theoretical spectrum for 40:60 ratio of AU to GC pairs. Theoretical curves are computed from linear combination of individual hypochromism spectra of poly(rA):poly(rU) and poly(rG):poly(rC) (Fresco et al., 1963).

a heat–cool cycle that may have been too rapid to allow for establishment of thermal equilibrium at each stage of the melt, and the other study (Maruyama et al., 1979) was conducted in very low ionic strength buffer in which single-stranded and less stable helical segments may be absent. The present results thus suggest that yeast 5S RNA contains two distinguishable stacked regions: approximately half the bases are stacked in (thermally stable) double-helical segments and the other half in single-stranded or less stable double-stranded segments.

Figure 2 shows the UV–melting profiles for yeast 5S RNA monitored at 260 nm (A_{260} is relatively more sensitive to AU stacking) and 280 nm (A_{280} is more sensitive to GC stacking) (Fresco et al., 1963; Van et al., 1977). Since these two melting profiles essentially coincide, it appears that yeast 5S RNA contains no predominantly AU- or GC-rich regions.

Figure 3 (solid line) shows the experimental yeast 5S RNA normalized UV hypochromism spectrum (i.e., difference in absorption between 20 and 85 °C over the 230–300-nm range). Since the separate normalized hypochromism spectra for poly(rG):poly(rC) and poly(rA):poly(rU) are markedly different (Fresco et al., 1963), linear combinations of these two curves may be used to estimate the relative proportions of GC and AU pairs in the experimental 5S RNA spectrum (see Figure 1). The best-fit simulation for yeast 5S RNA is for 60% GC and 40% AU, in which only these two types of base

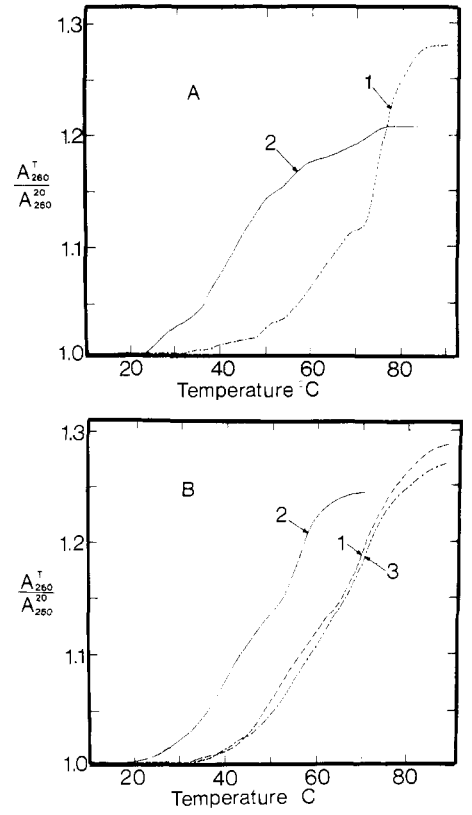

FIGURE 4: Experimental ultraviolet absorption–melting profiles for *S. cerevisiae* $tRNA^{Phe}$ (A) and 5S RNA (B) in the presence (1) and absence (2) of Mg^{2+}. Curve 3 in (B) is for 5S RNA renatured after removal of Mg^{2+}, using 10 mM phosphate, pH 7, 100 mM NaCl, and 10 mM Mg^{2+}. Mg^{2+}-containing samples contained 10 mM phosphate, pH 7, 100 mM NaCl, and 10 mM Mg^{2+}. Samples from which Mg^{2+} had been removed contained 10 mM phosphate, pH 7, 100 mM NaCl, and 1 mM EDTA.

pairs are considered. Since this procedure neglects single-stranded contributions to denaturation, nearest-neighbor effects, end of helix effects, and GU pair contributions, the experimental curve can be accurately simulated only in the 260–290-nm range and the resulting GC/AU ratio of 3:2 is probably only precise to ±10%.

The number of base pairs in yeast 5S RNA may be estimated as follows. If 100% of the bases were paired, a total hypochromism of about 0.30 would be expected (Boedtker & Kelling, 1967). Moreover, other tRNAs and 5S RNAs typically contain ~10% single-stranded contribution to the observed total hypochromism (Cantor, 1968; Boedtker & Kelling, 1967). Thus, an upper limit to the possible number of yeast 5S RNA base pairs in the presence of Mg^{2+} can be computed from the observed percentage of maximum possible hypochromism: $[(0.22 - 0.02)/0.30] \times 100 = 66\%$ of the 120 bases (i.e., 80 bases), corresponding to *40 base pairs*. The actual number is probably somewhat less (see NMR results).

(2) Mg^{2+} Absent. Normalized experimental UV–melting profiles for $tRNA^{Phe}$ in the presence and absence of Mg^{2+} are compared in Figure 4A and for yeast 5S RNA in Figure 4B. Mg^{2+} was actively removed by heat and EDTA treatment (see Experimental Section) in the Mg^{2+}-deficient samples in order to eliminate any effects from residual Mg^{2+} tightly held in the native (low temperature) structure. In addition, sample ionic strength was deliberately maintained at a near-physiological level in order to prevent unfolding of the structure due to too low ionic strength. Finally (Figure 4B), the melting profile of a Mg^{2+}-deficient sample can be reversibly restored by a Mg^{2+} replenishment procedure (see Experimental Section),

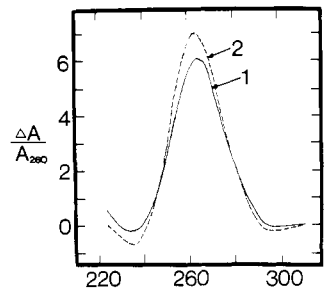

FIGURE 5: Normalized circular dichroism spectra for *S. cerevisiae* 5S RNA(—) and $tRNA^{Phe}$ (---). Buffer contained 10 mM phosphate, pH 7, 100 mM NaCl, and 10 mM Mg^{2+}.

Table II: Circular Dichroism Parameters for Yeast 5S RNA

RNA type	Mg^{2+}	λ_{max}[a] (nm)	$\Delta A/A_{260}$[b]
5S RNA	present	262.5	6.3×10^{-4}
	removed	263	6.1×10^{-4}
$tRNA^{Phe}$	present	261	6.7×10^{-4}
	removed	262.5	5.2×10^{-4}

[a] λ_{max} is the wavelength at the maximum dissymmetry ratio. [b] $\Delta A/A_{260}$ is the normalized maximum dissymmetry ratio. Both λ_{max} and $\Delta A/A_{260}$ are determined from CD spectra such as those in Figure 5, taken in the presence and absence of Mg^{2+}.

except for a slight loss in single-stranded hypochromism. It is thus possible to renature yeast 5S RNA almost completely, even after complete removal of Mg^{2+}. Hypochromism (H), half-melted temperature (T_m), and melting range (δ) values corresponding to the melting profiles of parts A and B of Figure 4 are given in Table I.

The data of parts A and B of Figure 4 show that the removal of Mg^{2+} leads to much more drastic structural changes for $tRNA^{Phe}$ than for 5S RNA. The $tRNA^{Phe}$ crystal structure (Holbrook et al., 1977; Jack et al., 1977) contains at least three to four strong Mg^{2+} binding sites that are critically positioned to stabilize the three-dimensional folding of the molecule. Thus, removal of these critical Mg^{2+} ions accounts for the 29 °C drop in melting temperature, 23% loss in base stacking, and a less concerted melting process (the increase in δ value on removal of Mg^{2+} suggests an increase in the extent of single-stranded stacking). For 5S RNA, on the other hand, removal of Mg^{2+} produces much less pronounced effects on the melting profile: 18 °C drop in T_m, 9% loss in hypochromism, and 12% decrease in δ value. In addition, the shape of the 5S RNA melting curve remains constant and biphasic on removal of Mg^{2+}.

Circular Dichroism Spectra of Yeast 5S RNA and $tRNA^{Phe}$. (1) 10 mM Mg^{2+} Present. Figure 5 consists of normalized CD spectra of Mg^{2+}-containing yeast 5S RNA and $tRNA^{Phe}$, with the λ_{max} (wavelength at maximum dissymmetry ratio) and $\Delta A/A_{260}$ (normalized maximum dissymmetry ratio) values listed in Table II. Previous work (Cantor, 1968) showed that a blue shift in λ_{max} and an increase in $\Delta A/A_{260}$ correspond to an increase in helicity. The present CD data therefore establish only a 6% higher helical content for $tRNA^{Phe}$ than for yeast 5S RNA. Since most of the bases in $tRNA^{Phe}$ are contained in two long helical segments (Sussman et al., 1978), yeast 5S RNA must also contain major helical segments and a highly ordered solution structure. The slightly lower helical content of 5S RNA (compared to $tRNA^{Phe}$) can be ascribed to the necessary bulges in the base-paired arms of the secondary structure and possibly to a less extensive tertiary structure than in tRNA. These bulges presumably interrupt the continuous helix and thus reduce the CD intensity.

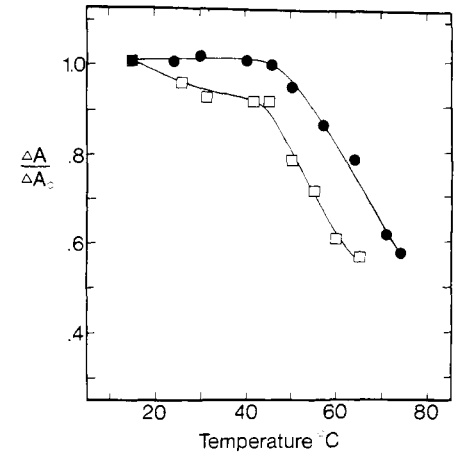

FIGURE 6: Normalized maximum dissymmetry ratio vs. temperature for *S. cerevisiae* 5S RNA in the presence (●) and absence (□) of Mg^{2+}. Buffers were as in Figure 4B. ΔA and ΔA_0 were determined from the CD band maximum value at $\lambda = \lambda_{max}$.

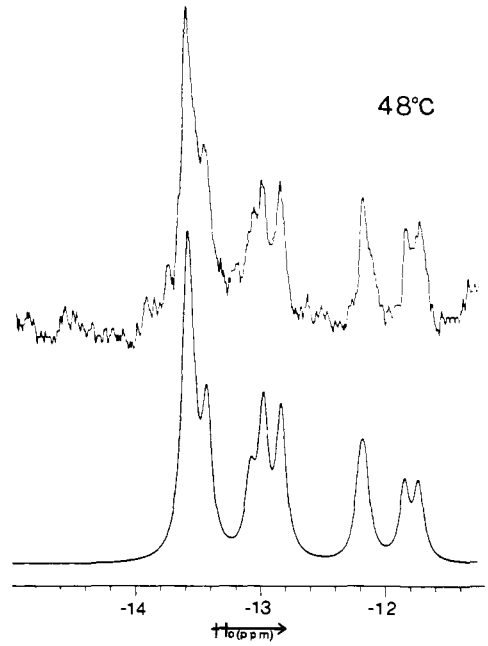

FIGURE 7: 360-MHz ^1H NMR spectrum of *S. cerevisiae* 5S RNA at 48 °C (upper curve) and the theoretical spectrum (bottom curve) constructed from a sum of 17 Lorentzian lines of equal intensity and equal line width (each 40 Hz wide at half-maximum height). Chemical shifts are referred to DSS at zero. Buffer contained 10 mM cacodylate, pH 7, and 100 mM NaCl.

(2) Mg^{2+} Absent. Figure 6 shows normalized CD–melting profiles for yeast 5S RNA in the presence and absence of Mg^{2+}. Table II lists λ_{max} and $\Delta A/A_{260}$ values for 5S RNA and $tRNA^{Phe}$ at low temperature in the presence and absence of Mg^{2+}. As in the case of UV absorption, the removal of Mg^{2+} leads to much bigger changes in the CD spectrum of $tRNA^{Phe}$ than of 5S RNA; $\Delta A/A_{260}$ decreases by some 22% on removal of Mg^{2+} from $tRNA^{Phe}$, but only 3% for 5S RNA. Thus, the helical content of 5S RNA is evidently not significantly reduced by removal of Mg^{2+}.

360-MHz ^1H NMR Spectra of Yeast 5S RNA. Figures 7–9 show the 360-MHz ^1H NMR spectra of yeast 5S RNA at 48, 41, 33, and 25 °C, all in the absence of Mg^{2+}. Using a procedure previously demonstrated successfully for the 360-MHz ^1H NMR spectra of a large number of tRNAs (Reid & Hurd, 1977), we first simulated the experimental spectrum at 48 °C (Figure 7) by varying the number and positions of theoretical

Table III: Structural Properties of Yeast 5S RNA

property	exptl value	value predicted by secondary structural model: Vigne & Jordan (1977)	Nishikawa & Takemura (1978)	Cloverleaf
[GC/(GC + AU)] × 100 (%)	60[a]	58	56	55
GU pairs	–	2	4	5
total pairs	≤40[b] ≥35[c]	21	38	34
% of U bases paired	65[d]	36	68	64

[a] From UV absorption data of Figure 3. [b] From Figure 1 (see text). [c] From Figure 8. [d] From Raman data (Luoma & Marshall, 1978b).

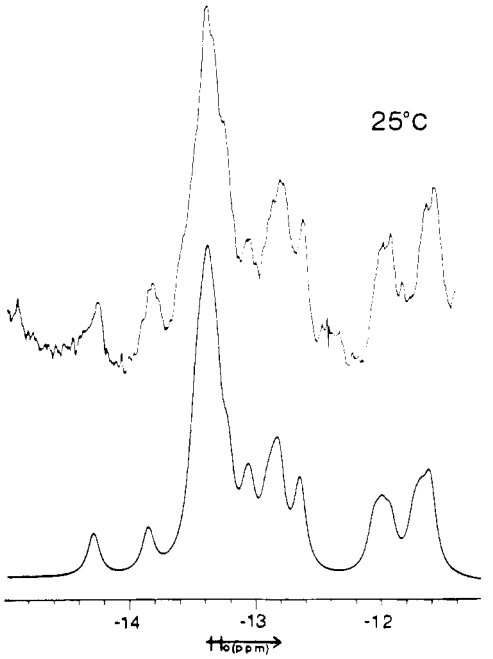

FIGURE 8: 360-MHz ^{1}H NMR spectra of *S. cerevisiae* 5S RNA. Top: experimental spectrum at 25 °C (chemical shift scale and buffer as in Figure 7). Bottom: theoretical spectrum constructed from a sum of 32 Lorentzian lines of equal width (each 44 Hz wide at half-maximum height), 17 of which have the same relative positions as in Figure 7 (see text).

individual Lorentzian lines of equal width (40 Hz) and intensity to give a best fit to the experimental spectrum. Then, in order to simulate the 25 °C experimental spectrum (Figure 8), we assigned the 17 lines identified at 48 °C the same relative chemical shifts (and a new common line width of 44 Hz), and additional Lorentzians (each 44 Hz wide) were added and shifted until the experimental and simulated spectra agreed. The yeast 5S RNA 360-MHz ^{1}H NMR spectrum at any temperature is much better resolved in the absence (Figures 7–9) than in the presence (not shown) of Mg^{2+}; a similar effect has been observed by many workers for tRNAs. From similar simulations on Mg^{2+}-containing yeast 5S RNA samples, we estimate that an additional three to four protons (corresponding to an additional 3–4 base pairs) are present at 25 °C in the presence of Mg^{2+}.

Discussion

Experimental Properties and Proposed Secondary Structural Models for Yeast 5S RNA. The present optical and NMR results lead to the following properties of the yeast 5S RNA solution structure: (i) 35–40 total base pairs in the native (25 °C in the presence of Mg^{2+}) structure; (ii) a 60:40 ratio of GC pairs to AU pairs; (iii) significant single-stranded stacking; (iv) minor dependence on Mg^{2+} (number of base pairs increases by only 3–4 on addition of Mg^{2+} to yeast 5S

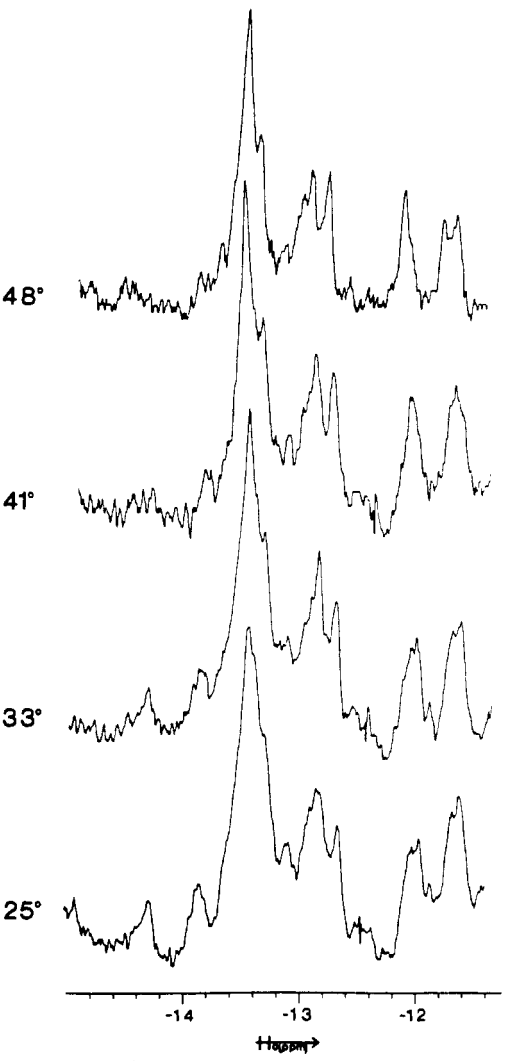

FIGURE 9: 360-MHz ^{1}H NMR spectra of *S. cerevisiae* at four temperatures in the absence of Mg^{2+}.

RNA from which Mg^{2+} was previously removed); (v) somewhat less helical content than native yeast $tRNA^{Phe}$; (vi) essentially reversible renaturation to native form by adding Mg^{2+} and heating 5S RNA from which Mg^{2+} had previously been removed; (vii) slightly less stable structure than native yeast $tRNA^{Phe}$.

Figure 10 and Table III show that the cloverleaf model (Luoma & Marshall, 1978a,b) can accommodate all the presently reported physical properties, as well as independently determined enzymatic cleavage susceptibility (Nichols & Welder, 1979), chemical modifications (Nishikawa & Takemura, 1978), and Raman intensity patterns (Luoma & Marshall, 1978b).

Specifically, both the UV-melting profiles and the CD spectra indicate a large number of base pairs (≤40) and ex-

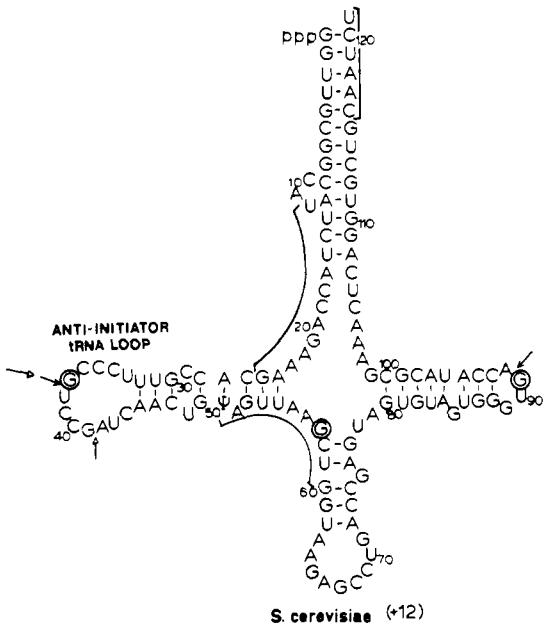

FIGURE 10: Cloverleaf model for secondary structure of *S. cerevisiae* 5S RNA. Arrows denote sites of initial cleavage by T_1 RNase (→) (Vigne et al., 1973) and T_2 RNase (→) (Vigne et al., 1973). Circled residues are those that are ≥50% modified by kethoxal (Nishikawa & Takemura, 1978), and bracketed segments are susceptible to single-strand-specific S_1 nuclease digestion (Nichols & Welder, 1979).

tensive helical content. The Mg^{2+} dependence of the optical data (see below) points to a substantial single-stranded contribution to the overall helical content and base stacking. This contribution might well arise from the "stem" region of the cloverleaf (Figure 10), in which bases 16–23 and 101–108 are shown unpaired, but could be stacked in single-stranded segments.

The 360-MHz ^1H NMR results unequivocally demonstrate the presence of 32 ± 2 base pairs in native yeast 5S RNA from which Mg^{2+} has been removed, since there will be 1 base pair corresponding to each of the 32 peaks that were needed to reproduce the experimental spectrum in the chemical shift range from −11.6 to −15.0 ppm from DSS. [Each GU pair gives two peaks, but only one of these should be found downfield of −11.6 ppm (Geerdes & Hilbers, 1979).] The slight increase in line width (from 40 to 44 Hz) on cooling the Mg^{2+}-free 5S RNA from 48 to 25 °C is probably due to a corresponding increase in solution viscosity. An additional increase in line width on addition of Mg^{2+} probably reflects a somewhat more rigid conformation in the presence of Mg^{2+}. Although simulation of the 5S RNA spectrum in the presence of Mg^{2+} is less reliable (because of broader lines and poorer resolution), we estimate that only 3–4 additional base pairs are observable. Combining this lower limit (since rapid exchange between base pair protons and solvent may broaden or eliminate some NMR peaks) with the upper limit from the (optical) hypochromicity, we conclude that 35–40 total base pairs are present in the native yeast 5S RNA solution structure.

Finally, application of Tinoco rules (Tinoco et al., 1973) to the cloverleaf model suggests that the stem and right arm should be most stable; these two regions contain 21 total base pairs (7 A:U, 10 G:C, and 4 G:U), in approximate agreement with the 17 base pairs observed at 48 °C (Figure 7) in the absence of Mg^{2+}.

The above results tend to rule out the Vigne & Jordan (1977) model, since it contains too few secondary pairs (see Table III). Moreover, the discrepancy cannot be due to a large number of tertiary pairs, because the UV hypochromism for yeast 5S RNA decreases only slightly on removal of Mg^{2+}, and the decrease in hypochromism for yeast $tRNA^{Phe}$ on removal of Mg^{2+} corresponds exactly to the disappearance of tertiary structure in that molecule.

The present results are also consistent with the model of Nishikawa & Takemura (1978), since its secondary pairing pattern is similar to the cloverleaf model (Luoma & Marshall, 1978b). However, S_1 nuclease digestion experiments favor the cloverleaf structure, since the region from 11–25 in the primary sequence is less involved in base pairing than in the Nishikawa and Takemura model.

Previous Studies. The present results differ from previous estimates of the number of base pairs in yeast 5S RNA based on optical (Maruyama et al., 1979) or ^1H NMR (Wong et al., 1972) results. The previous optical estimate was ~30 base pairs, for example, compared to the present 35–40. However, as acknowledged by those authors, their experiments were conducted at low ionic strength, so that some secondary structure may have already melted out. We suggest that their "melted" region may well correspond to the left-hand arm ("antiinitiator tRNA arm") of the cloverleaf, since it is the least stable region based on Tinoco rules (Tinoco et al., 1973). With regard to the previous NMR data (21 ± 2 pairs in the absence of Mg^{2+}; 28 ± 3 pairs in the presence of Mg^{2+} at 35 °C), there are several problems. First, the integration method based on external standards has since been shown to give estimates of base pairs that are too low by up to 6 base pairs (Reid & Hurd, 1977). Second, some base pairs at this temperature (35 °C) will be partially melted, making it very difficult to estimate the correct base pair number without simulation of the spectrum. Third, the signal-to-noise ratio and resolution at 220 MHz (the highest NMR frequency then available) are simply not sufficient to permit accurate interpretation, partly because of the high RNA concentration (at which aggregation may occur) required in those measurements. The present results are thus consistent with and more reliable than previous studies.

Comparison of Yeast 5S RNA and E. coli 5S RNA. As previously noted, *E. coli 5S RNA* can assume two distinct solution conformations: a native ("A") form that dominates in Mg^{2+}-containing buffers, and a denatured, chromatographically isolable ("B") form that can be generated by heating to 60 °C in the absence of Mg^{2+} and then recooling (Aubert et al., 1968; Richards et al., 1973; Burns et al., 1980). However, *S. cerevisiae* 5S RNA appears to show no such additional form, since the high-temperature CD and UV spectra change only slightly on removal of Mg^{2+}. Moreover, the 360-MHz ^1H NMR spectrum at 25 °C is the same before and after heating to 60 °C and changes only slightly on removal of Mg^{2+}. [In contrast, $tRNA^{Phe}$ shows gross changes in UV, CD, and NMR behavior on removal of Mg^{2+}.] If, as has recently been suggested (Weidner et al., 1977), a conformational change from one form of *E. coli* 5S RNA to another functions to help translocate tRNA at the ribosome, then the absence of other conformational forms of yeast 5S RNA would mean either that this mechanism does not operate in yeast or that different conditions will be required to produce the other yeast RNA form(s) (if they exist).

The present optical and NMR results, and previous Raman (Luoma & Marshall, 1978b) results, combine to give an accurate representation of the structural features of yeast 5S RNA in solution, at ionic strength resembling physiological conditions.

Acknowledgments

The authors thank Professor Gerd La Mar for his generous

provision of instrument time on the Nicolet-360 FT-NMR spectrometer at the University of California, Davis.

References

Appel, B., Erdmann, V. A., Stulz, J., & Ackermann, Th. (1979) *Nucleic Acids Res. 7*, 1043–1057.

Aubert, M., Scott, J. F., Reynier, M., & Monier, R. (1968) *Proc. Natl. Acad. Sci. U.S.A. 61*, 292–299.

Bear, D. G., Schleich, T., Noller, H. F., & Garrett, R. A. (1977) *Nucleic Acids Res. 4*, 2511–2526.

Boedtker, H., & Kelling, D. G. (1967) *Biochem. Biophys. Res. Commun. 29*, 758–766.

Burns, P. D., Luoma, G. A., & Marshall, A. G. (1980) *Biochem. Biophys. Res. Commun. 96*, 805–811.

Cantor, C. R. (1968) *Proc. Natl. Acad. Sci. U.S.A. 59*, 478–483.

Chen, M. C., Giege, R., Lord, R. C., & Rich, A. (1978) *Biochemistry 17*, 3134–3138.

Cramer, F., & Erdmann, V. A. (1968) *Nature (London) 218*, 92–93.

Erdmann, V. A. (1976) *Prog. Nucleic Acids Res. Mol. Biol. 18*, 45–90.

Fox, J. W., & Wong, E. P. (1978) *J. Biol. Chem. 253*, 18–20.

Fresco, J. R., Klotz, L. C., & Richards, E. G. (1963) *Cold Spring Harbor Symp. Quant. Biol. 28*, 83–90.

Geerdes, H. A. M., & Hilbers, C. W. (1979) *FEBS Lett. 107*, 125–128.

Gillam, I., Millward, S., Blew, D., von Tigerstrom, M., Wimmer, E., & Tener, G. M. (1967) *Biochemistry 6*, 3043–3056.

Gray, P. N., & Saunders, G. F. (1973) *Arch. Biochem. Biophys. 156*, 104–111.

Holbrook, S. R., Sussman, J. L., Warrant, R. W., Church, G. M., & Kim, S.-H. (1977) *Nucleic Acids Res. 4*, 2811–2820.

Holmes, W. M., Hurd, R. E., Reid, B. R., Rimerman, R. A., & Hatfield, G. W. (1975) *Proc. Natl. Acad. Sci. U.S.A. 72*, 1068–1071.

Jack, A., Ladner, J. E., Rhodes, D., Brown, R. S., & Klug, A. (1977) *J. Mol. Biol. 111*, 315–329.

Kearns, D. R., & Wong, Y. P. (1974) *J. Mol. Biol. 87*, 755–774.

Levy, J., & Rialdi, G. (1972) *Biochemistry 11*, 4145–4152.

Levy, J., Rialdi, G., & Biltonen, R. (1972) *Biochemistry 11*, 4138–4144.

Luoma, G. A., & Marshall, A. G. (1978a) *Proc. Natl. Acad. Sci. U.S.A. 75*, 4901–4905.

Luoma, G. A., & Marshall, A. G. (1978b) *J. Mol. Biol. 125*, 95–105.

Marshall, A. G., & Smith, J. L. (1980) *Biochemistry* (in press).

Maruyama, S., Tatsuki, T., & Sugai, S. (1979) *J. Biochem. (Tokyo) 86*, 1487–1494.

Monier, R. (1974) in *Ribosomes* (Nomura, M., Tissieres, A., & Lengyel, P., Eds.) pp 141–168, Cold Spring Harbor Laboratory, Cold Spring Harbor, NY.

Nazar, R. N., Sprott, G. D., Matheson, A. J., & Van, N. J. (1978) *Biochim. Biophys. Acta 521*, 288–294.

Nichols, J. L., & Welder, L. (1979) *Biochim. Biophys. Acta 561*, 445–451.

Nishikawa, K., & Takemura, S. (1978) *J. Biochem. (Tokyo) 84*, 259–266.

Noller, H. F., & Garrett, R. A. (1979) *J. Mol. Biol. 132*, 621–648.

Redfield, A. G., Kunz, S. D., & Ralph, E. K. (1975) *J. Magn. Reson. 19*, 114.

Reid, B. R., & Robillard, G. T. (1975) *Nature (London) 257*, 287–291.

Reid, B. R., & Hurd, R. E. (1977) *Acc. Chem. Res. 10*, 396–402.

Richards, E. G., Geroch, M. E., Simpkins, H., & Lecanidou, R. (1972) *Biopolymers 11*, 1031–1039.

Richards, E. G., Lecanidou, R., & Geroch, M. E. (1973) *Eur. J. Biochem. 34*, 262–267.

Riesner, D., Maass, G., Thiebe, R., Phillipsen, P., & Zachau, H. G. (1973) *Eur. J. Biochem. 36*, 76–88.

Romer, R., Riesner, D., & Maass, G. (1970) *FEBS Lett. 10*, 352–357.

Rubin, G. M. (1973) *J. Biol. Chem. 248*, 3860–3875.

Scott, J. F., Monier, R., Aubert, M., & Reynier, M. (1968) *Biochem. Biophys. Res. Commun. 33*, 794–800.

Sprinzl, M., Wagner, T., Lorenz, S., & Erdmann, V. A. (1976) *Biochemistry 15*, 3031–3039.

Sussman, J. L., Holbrook, S. R., Warrant, R. W., Church, G. M., & Kim, S.-H. (1978) *J. Mol. Biol. 123*, 607–630.

Swarz, U., Menzel, H. M., & Gassen, H. G. (1976) *Biochemistry 15*, 2484–2490.

Tinoco, I., Jr., Borer, P. N., Dengler, B., Levine, M. D., Uhlenbeck, O. C., Crothers, D. M., & Gralla, J. (1973) *Nature (London), New Biol. 246*, 40–41.

Van, N. F., Nazar, R. N., & Sitz, T. O. (1977) *Biochemistry 16*, 3754–3759.

Vigne, R., & Jordan, B. R. (1977) *J. Mol. Evol. 10*, 77–86.

Vigne, R., Jordan, B. R., & Monier, R. (1973) *J. Mol. Biol. 76*, 303–311.

Weidner, H., Yuan, R., & Crothers, D. M. (1977) *Nature (London) 266*, 193–194.

Wittman, H. G. (1979) *Can. J. Biochem. 57*, 1251–1261.

Wong, Y. P., Kearns, D. R., Reid, B. R., & Shulman, R. G. (1972) *J. Mol. Biol. 72*, 741–749.

Wool, J. G. (1979) *Annu. Rev. Biochem.*, 719–754.